Bulgarian Chemical Communications, Volume 52, Special Issue E (pp. 62 - 67) 2020

Electrochemical deposition of Sb_2Se_3 thin films semiconductor from tartaric acid solution

V. A. Majidzade*, A. Sh. Aliyev, D. B. Tagiyev

Institute of Catalysis and Inorganic Chemistry named after acad.M.Nagiyev, Azerbaijan National Academy of Sciences, H.Javid ave., 113, AZ 1143, Baku, Azerbaijan

Received November 16, 2019; Accepted January 27, 2020

The proffered work has been dedicated to the electrochemical deposition of Sb-Se layers from tartaric acid as an electrolyte. In the course of research, the cyclic voltammetric polarization curves have been diagrammed by the potentiodynamic method. Sb-Se films have been deposited on different metals by potentiostatic and galvanostatic methods. The analysis of polarization curves and X-ray analysis of obtained samples indicate that Sb_2Se_3 was formed as a result of our research.

Keywords: Antimony-selenide, electrodeposition, polarization, tartaric acid, semiconductive layers

INTRODUCTION

Binary chalcogenide semiconductors have attracted considerable attention in the past few years owing to their applications in photoelectrochemical devices, optoelectronic devices, switching devices, thermoelectric coolers, decorative coatings etc [1-12]. The aim of the production of these thin layers is to enhance stability and effectiveness of solar batteries **[**13].

Antimony Triselenide (Sb_2Se_3) is a member of the V-VI semiconductor family [14-23]. It is a staggered layered compound, direct band gap semiconductor with orthorhombic crystal structure [24]. Sb_2Se_3 is also a promising light absorber material [25-27]. Excellent optoelectronic properties such as high absorption coefficient (>105 cm^{-1}), low band gap (ranging from 1.1-1.3 eV) suitable for visible light harvesting and p-type conductivity makes it an ideal candidate for solar cell applications. In addition to it, low material cost, abundant supply and relatively low toxicity constituents are some of the added advantages suitable for photovoltaics [28-30].

Currently, photoelectrochemical splitting of water is an attractive and sustainable way to generate hydrogen, which can be used to maintain fuel economy [31-33], and photoelectrodes in PEC elements play a crucial role in the solar-hydrogen process (STH) conversion efficiency [34].

Sb_2Se_3 has received a lot of attention in this area - for thermoelectric, photovoltaic and energy storage [35-36] applications owing to its earth abundance, non-toxicity in comparison toxicity to elemental selenium, single phase (indicating the phase and defects of Sb_2Se_3 can be easy to control), favorable band gap value (1.1~ 1.2 eV) [37-39].

Sb_2Se_3 semiconductive layers are obtained using various methods: vacuum thermal evaporation [40], rapid thermal evaporation [41], chemical bath deposition [42, 43], spin coating [44], electrodeposition [45], arrested precipitation technique [46], pulsed laser deposition [47], photoelectrochemical deposition [48] and etc.

Some researchers **[**17**,** 18] got thin layers of Sb_2Se_3 with 200-720 nm in thickness using thermal evaporation via deposition on the glass substrate. The effect of the thickness of these amorphous layers to their structure, morphology and optical properties has been studied. The optical adsorption of Sb_2Se_3 layers is related to indirect adsorption gap, whereas the change of width of the forbidden band is explained by the existence of structural defects and irregularity in the chalcogenide systems. The result of optical adsorption indicated that the regularity of layer structures increases with their thickness. Authors second essential goal was a search of the mechanism of transforming of thin-layered Sb_2Se_3 into the memory cell.

Thin-layered Sb_2Se_3 has been obtained with via electrodeposition on the stainless steel and glass electrodes in the nonaqueous medium **[**19**].** The layers of higher quality can be obtained from 0.05M of electrolyte prepared from $SbCl_3$ and SeO_2 components taken in 1:1 ratio. According to the result of SEM analysis, the semiconductive Sb_2Se_3 layers cover the electrode surface totally and the width of the forbidden band (energy gap) is 1.195 eV. Some researchers have attempted to synthesize

* To whom all correspondence should be sent.
E-mail: vuska_80@mail.ru

antimony-selenide of different shapes. They proved that there were homopolar (Se-Se) and heteropolar (Sb-Se) bonds in the obtained nanolayered [20], nanospheric [21] and nanowire layers by mean of Raman Spectroscopy.

Some investigations showed that [22] the deposited films of Sb_2Se_3 with different thicknesses at a rate of 30 Å s, and at room temperature were found to have an amorphous structure. The electric resistance of these layers on the silver electrodes increases with the increase of the thickness of the layer up to 370.8 nm, gets the maximal point, but after this point, it decreases. The specific resistance for every thickness decreases with increasing of temperature. Thin layers of Sb_2Se_3 were deposited using electrochemical atomic layer epitaxy (ALE) [23]. From analyzing literature related to the matter under investigation it is shown that the most effective method to deposit Sb and Se simultaneously is electrochemical. There are rare data about the electrochemical synthesis of Sb-Se, So it needs more information and experiments to clear the view. Thus, throughout the work, the thin-layered semiconductive Sb-Se has been obtained by the electrochemical method.

EXPERIMENTAL

The codeposition of antimony and selenium by the electrochemical way has been achieved as follows: tartaric acid was dissolved in distilled water to prepare under-investigated electrolyte solution, then SbOCl salt and selenite acid (H_2SeO_3) was dissolved in tartaric acid solution, separately. The compositions of the obtained electrolytes consist of 0.05 mol/L SbOCl+ 0.007 mol/L $C_4H_6O_6$ (tartaric acid) and 0.05 mol/L H_2SeO_3 + 0.007 mol/L $C_4H_6O_6$. The polarization curves have been recorded using IVIUMSTAT Electrochemical İnterface Potentiostat. A three-electrode electrochemical cell was used. The working electrodes here were Pt 2 mm^2 surface area and Ni with 2 cm^2 surface area. Silver electrode (Ag/AgCl) was used as a comparative (reference) electrode. Pt sheet of 4 cm^2 surface area was used as an auxiliary electrode. Throughout the electrolysis process, the temperature of the electrolyte solution was regulated by UTU – 4 universal ultra-thermostat. The phase composition of the obtained thin layers was studied with "D2 Phazer" XRay Phase Analyzer of "Bruker" company (CuK_α; Ni filter). The morphology and chemical element composition of samples were analyzed by scanning electron microscopy (SEM) "Carel Zeiss Sigma". The adhesion of thin films to the surface of the electrode is determined by the method of lattice cuts [49] and bending of the electrode at an angle of 90°.

on prepared samples using a ruler At least 5 parallel and 5 perpendicular cuts at a distance of 1 or 2 mm from each other are made. In this case, a lattice of squares of the same size is formed on the surface. After applying the grating, the coating surface is cleaned with a brush from exfoliated pieces of film and adhesion is evaluated on a four-point scale: 1 point - the edges of the incisions are smooth, there are no exfoliated pieces of coating; 2 points - peeling of the coating with 5% of the surface of the lattice;

3 points - peeling of the coating from 35% of the surface of the grating; 4 points - peeling of the coating with more than 35% of the surface of the grating;

Before starting experiment required Pt is chemically polished in concentrated sulfuric acid and hydrogen peroxide solution, and then washed with distilled water. The Ni electrodes, at first, polished electrochemically in concentrated HNO_3 acid, then refurbished in a solution consists of H_2SO_4, H_3PO_4 and citric acids (T = 293-303K, i = 50 A/dm^2, τ =180 sec.). Finally, Ni electrodes are washed with distilled water.

RESULTS AND DISCUSSION

It is known that for codeposition of any two components by the electrochemical method, at first, kinetics and mechanism of deposition of these components from the taken electrolyte and various patterns should be studied separately. The deposition process of both antimony [50, 51] and selenium [52] from tartaric acid has been investigated by our team. The electrochemical cathodic reduction processes of both components were studied; the optimal conditions were defined and investigated of the codeposition process. The kinetics and mechanisms of the electrochemical deposition of antimony and selenium from tartaric acid have been investigated separately. The cyclic voltammetric polarizations of the codeposition process of Sb and Se on Pt electrode were achieved by the potentiodynamic method, as given in Fig. 1. It seems from this figure, that codeposition process of Sb and Se layers is mono-stage and occurs within the potential range of -0.42 – (-0.7) V. The transforming processes of SeO_3^{2-} ions into Se^0, then of electroreduced into Se^{2-} ions occurred at a potential starting from -0.42 V to 0.55 V [52]. After that, the obtained adsorbed Se^{2-} ions on the electrode surface joined with Sb^{3+} ions in solution forming Sb-Se thin films. As a result, it can be noticed that the surface of the electrode is covered with a black layer. After a potential of –0.7 V the

hydrogen gas is released, therefore simultaneous process has been studied up to this point of potential.

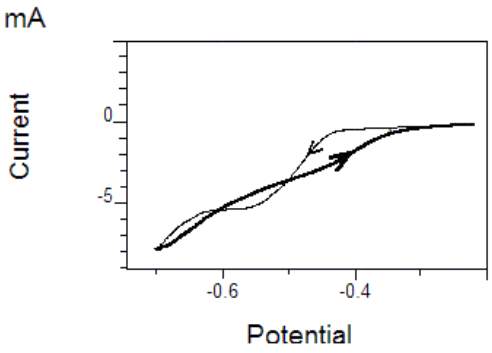

Fig.1. The cyclic polarization curve of the co-deposition process of Sb-Se layers on the Pt electrode immersed in an electrolyte consists of: 0.05 (mol/L) SbOCl + 0.05 (mol/L) H_2SeO_3 + 0.007 (mol/L) $C_4H_6O_6$, at T = 298 K, and E_V = 0.03 V/s.

The result of X-Ray Phase Analysis of the electrodeposited Sb-Se layers on Pt electrode shows that through the co-electrodeposition process, the Sb_2Se_3 is obtained at these conditions. It is observed that the electrodeposited thin layers of Sb_2Se_3 are black in color, and there is a strong adhesion (2 point) between the substrate surface and the obtained compound. Depending on the condition of the electrochemical process, the composition and quality of the obtained thin layers are varied dissimilarly (Table 1).

As seen from Table 1, the quantity of components in deposited layers increases statutorily with increasing their concentration that included in an electrolyte′s contents. Also, it is observed that the color of layers is changed from golden-red to dark black.

Table 1. The composition and quality of the obtained Sb-Se thin layers depending on the condition of the electrochemical process

№	The composition of solution, (mol/L)		The composition of the layer, mass %		Thermal processing,	The appearance of the layer
	SbOCl	H_2SeO_3	Sb	Se	T, K	
1.	0.01	0.09	15.2	84.8	673	Golden-red, rough, amorphous
2.	0.05	0.05	62.26	37.74	723	Black-red, smooth, crystalline
3.	0.09	0.01	82.6	17.4	703	Dark black, crystalline, smooth
4.	0.01	0.09	23.7	76.3	293	Golden-red, smooth, amorphous
5.	0.05	0.05	48.27	51.73	293	Black-red, low crystalline, smooth
6.	0.09	0.01	70.7	29.3	293	Dark black, crystalline, rough

On the other hand, it can be noticed from Table 1 that the quantity of Sb is more in layers that are exposed to thermal processing under argon atmosphere. It looks like thermal evaporation of Se after 673K temperature. The effect of different factors (temperature, the concentration of components, the rate of potential and etc.) to co-electrodeposition process of the semiconductive Sb_2Se_3 compound have been clarified [53].

The essential effective factor – the temperature has been studied. The cyclic voltammetric polarization curves via the potentiodynamic method on the Ni electrode were given in figure 2. The experiments were carried out within the range of 298-358 K. As is seen from the curves of Fig. 2, it can be observed that with an increase in the temperature, the deposition process accelerates. The temperature increment stimulates obtaining of crystalline layers. But this process continues up to about 338-343 K temperature interval. Upwards of 343 K temperatures the quality, adhesion, smoothness, composition, and crystallinity of obtaining layers decrease.

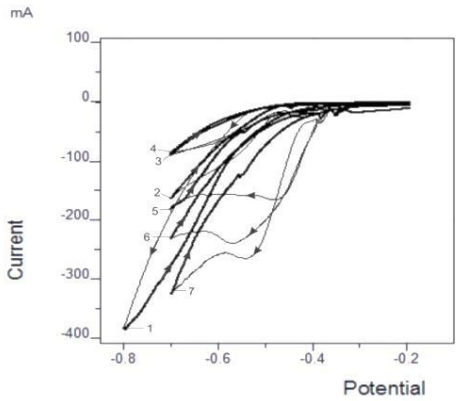

Fig. 2. The effect of temperature to co-deposition process of Sb-Se layers on the Pt electrode**.** Electrolyte composition (mol/L): 0.05 SbOCl + 0.05 H_2SeO_3 + 0.007 $C_4H_6O_6$. 1- 298K, 2- 308K, 3- 318K, 4- 328K, 5- 338K, 6- 348K, 7- 358K. E_V = 0.03 V/s.

The effect of the other main factor – concentration to the co-deposition process has been studied by both potentiodynamic and galvanostatic methods. Some of the outcomes were given in Table 1. Results show that stochiometric semiconductive layers are attained from 0.05 mol/L concentration of both components.

Table 2. The effect of temperature to co-deposition process of Sb-Se by electrochemical method according to the result of SEM analysis. Electrolyte (mol/L): 0.05 SbOCl + 0.05 H_2SeO_3 + 0.007 $C_4H_6O_6$, E_V = 0.03 V/s.

№	T, K	The composition of the layer, %		The appearance of the layer
		Sb	Se	
1.	308	27.25	72.75	Golden-red, amorphous, rough
2.	318	15.63	84.37	Reddish-black, small crystalline, rough
3.	328	18.57	81.43	Black, crystalline, smooth
4.	338	26.07	73.93	Dark-black, crystalline, smooth
5.	348	12.93	87.07	Dark-black, small crystalline, rough

Therefore, this concentration is optimal to get Sb_2Se_3. As seen from Fig. 3, the cyclic polarization curves of components within 0.025 - 0.09 mol/L concentration interval were given. It is observed from polarization curves that with increasing of concentration of SbOCl in the electrolyte, the co-deposition potential is displaced from - 0.72 V to - 0.38 V. It means that the co-deposition process is displaced to the more positive region with increasing of concentration.

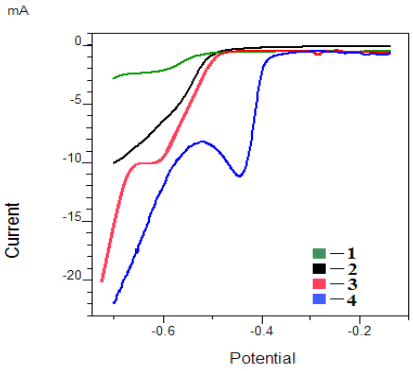

Fig. 3. The effect of the concentration of the components on the co-deposition process of Sb-Se via potentiodynamic method on the Pt electrode. Electrolyte composition (mol/L): 1- 0.025 SbOCl + 0.075 H_2SeO_3 + 0.007 $C_4H_6O_6$; 2- 0.05 SbOCl + 0.05 H_2SeO_3 + 0.007 $C_4H_6O_6$; 3- 0.075 SbOCl + 0.025 H_2SeO_3 + 0.007 $C_4H_6O_6$; 4- 0.09 SbOCl + 0.01 H_2SeO_3 + 0.007 $C_4H_6O_6$, at E_V = 0.03 V/s, and T= 298K.

The effect of the scan rate of potential to the co-deposition process has been also studied within 0.005-0.2 V/s interval (Fig. 4).

The experiment was carried out by potentiodynamic method via recording the cathodic polarization curves. From polarization curves, it is obvious that the increase in the scan rate of potential enables the co-deposition process to occur in the more cathodic potential region. It is important supremacy of the electrochemical process.

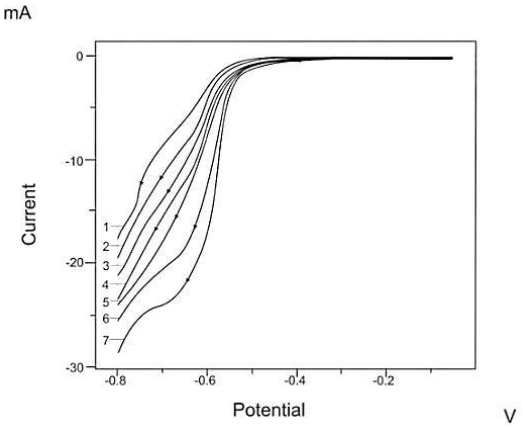

Fig. 4. The effect of the scan rate variation to the co-deposition process of Sb-Se via potentiodynamic method on the Pt electrode. Electrolyte composition (mol/L): 0.05 SbOCl + 0.05 H_2SeO_3 + 0.007 $C_4H_6O_6$; E_V (V/s): 1- 0.005; 2- 0.01; 3- 0.03; 4- 0.05; 5- 0.08; 6- 0.12; 7- 0.2. T= 298K.

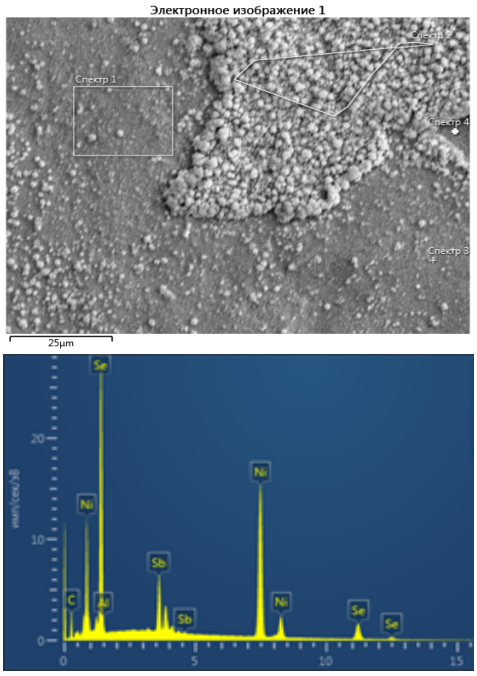

Fig. 5. SEM and EDX of the electrodeposited thin-layered Sb-Se on the Ni electrode. At the electrolyte composition of 0.05 mol/L SbOCl + 0.05 mol/L H_2SeO_3 + 0.007 mol/L $C_4H_6O_6$ at T= 338K.

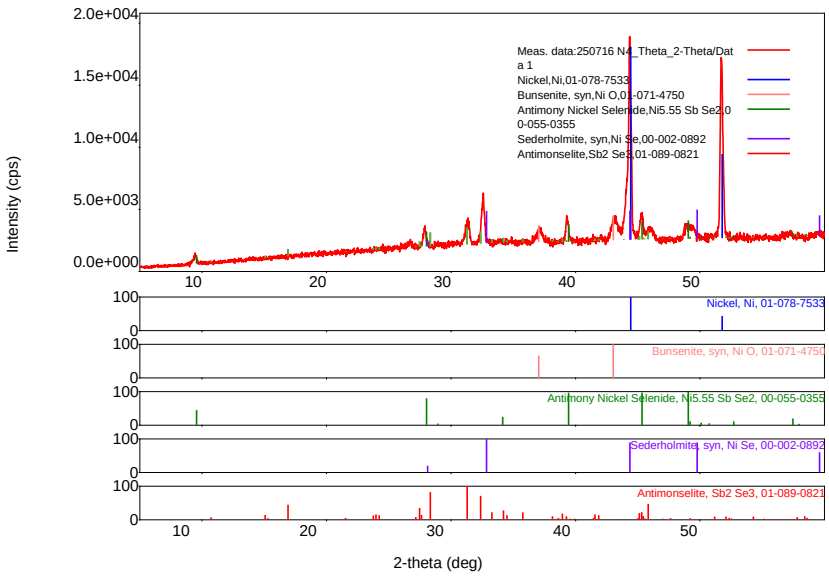

Fig. 6. X-Ray Phase Analysis of Sb-Se thin layers of the co-electrodeposited from electrolyte 0.05 mol/L SbOCl + 0.05 mol/L H_2SeO_3 + 0.007 mol/L $C_4H_6O_6$ on the Ni electrode, at T= 298K.

As a result of the accomplished investigation, the composition of electrolyte and electrolytic condition for obtaining of thin layers of the Sb_2Se_3 compound by electrochemical method were detected as follow: at the electrolyte composition of 0.05 mol/L SbOCl + 0.05 mol/L H_2SeO_3 + 0.007 mol/L $C_4H_6O_6$, E_V = 0.03 V/s, and T= 298K. The X-Ray Phase and SEM analysis of the obtained Sb_2Se_3 compound on Ni electrode confirmed that it is close to stoichiometric composition. The outcomes of this analysis were given in Figures 5 and 6.

CONCLUSIONS

The electrochemical deposition process of semiconductive Sb-Se thin layers has been investigated by both galvanostatic and potentiodynamic methods. The effects of the different factors on the co-deposition process of Sb-Se thin layers have been studied. The composition of electrolyte and electrolytic condition for depositing of these layers were typically determined according to outcomes. The results of X-ray Phase and SEM analysis indicate that the electrodeposited compound with stoichiometric composition (Sb_2Se_3) can be via the co-deposition process at our optimal conditions.

REFERENCES

1. 1. N.S. Shinde, V.B. Prabhune, H.D. Dhaigude, C.D. Lokhande, V.J. Fulari, *Appl. Surf. Sci.*, **255**, 8688 (2009).
2. A.P. Torane, C.H. Bhosale, *Mater. Res. Bull.*, **38,** 847 (2003).
3. A.D.A. Buba, E.O. Ajala, D.O. Samson, *Asian Journal of Science and Technology*, **6,** 1146 (2015).
4. A.Sh. Aliyev, Sh.O. Eminov, T.Sh. Sultanova, V.A. Mejidzadeh, D.A. Kuliyev, D. Jalilova, D.B. Tagiyev, *Chemical Problems.* **2,** 139 (2016)
5. M. Luo, M. Leng, X. Liu, J. Chen, C. Chen, S. Qin, J. Tang, *Appl. Phys. Lett.*, **104**, 173904 (2014).
6. O. Rachel, M.N. Jessy, R.P. Usha, *J. Ovonic Res.* **6**, 259 (2010).
7. R.G. Sotelo Marquina, T.G. Sanchez, N.R. Mathews, X. Mathew, *Mater. Res. Bull.*, **90**, 285 (2017).
8. A.Sh. Aliyev, V.A. Majidzade, N.Sh. Soltanova, D.B. Tagiyev, V.N. Fateev, *Chemical Problems*, **2**, 178 (2018).
9. Y.H. Yeo, T.S. Oh, *Mater. Res. Bull.*, **58**, 54 (2014).
10. R. Vadapoo, S. Krishnan, H. Yilmaz, C. Marin, *Phys. Status Solidi B.*, **248**, 700 (2011).
11. G.M. Huseynov, N.A. Mammadova, H.A. Imanov, *Chemical Problems*, **3**, 329 (2017).
12. A.Sh. Aliyev, M. Elrouby, S.F. Cafarova, *Mat. Sci. Semicon. Proc.*, *32*, 31 (2015).
13. T.T. Ngo, S. Chavhan, I. Kosta, O. Miquel, H.I. Grande, R. Tena-Zaera, *Acs. Appl. Mater. Inter.*, **6**, 2843 (2014).
14. A. Shongalova, M.R. Correia, B. Vermang, J.M.V. Cunha, P.M.P. Salomé, P.A. Fernandes, *MRS Communic.*, 1 (2018).
15. K.W. Sun, C.-H. Yang, T.-Y. Ko, H.-W. Liu, *Pure Appl. Chem.*, **81**, 1511 (2009).
16. S.-S. Zhang, J.-M. Song, H.-L. Niu, C.-J. Mao, S.-Y. Zhang, Y.-H. Shen. *J. Alloy Compd.*, **585**, 40 (2014).
17. M. Malligavathy, R.T. Ananth Kumar, Das Chandasree, S. Asokan, D. Pathinettam Padiyan, *J. Non-Cryst. Solids*, **429**, 93 (2015).

18. X. Liu, J. Chen, M. Luo, M. Leng, Z. Xia, Y. Zhou, S. Qin, D.-J. Xue, L. Lv, H. Huang, D. Niu, J. Tang, *ACS Appl. Mater. Interface*, **6**, 10687 (2014).
19. A.P. Torane, C.H. Bhosale, *J. Phys. Chem. Solids.*, **63**, 1849 (2002).
20. Y. Lai, Z. Chen, C. Han, L. Jiang, F. Liu, J. Li, Y. Liu, *Appl. Surf. Sci.*, **261**, 510 (2012).
21. Y. Zhang, G. Li, B. Zhang, L. Zhang, *Mater. Lett.*, **58**, 2279 (2004).
22. F. Abd El-Salam, M.A. Afify, E. Abd El-Wahab, *Vacuum*, **44**, 1009 (1993).
23. Y. Chen, L. Wang, A. Pradel, A. Merlen, M. Ribes. M.-C. Record, *J. Solid State Electrochem.*, **19**, 2399 (2015).
24. X. Shi, X. zhang, Y. Tian, C. Shen, C. Wang, H.-J. Gao, *Appl. Surf. Sci.***, 258**, 2169 (2012).
25. Y.C. Choi, Y.H. Lee, S.H. Im, J.H. Noh, T.N. Mandal, W.S. Yang, S.I. Seok, *Adv. Energy Mater.*, **4**, 1301680 (2014).
26. Y.C. Choi, T.N. Mandal, W.S. Yang, Y.H. Lee, S.H. Im, J.H. Noh, S.I. Seok, *Angew. Chem. Int. Ed. Engl*.**, 53**, 1329 (2014).
27. Z. Kai, X. Ding-Jiang, T. Jiang, *Semicond. Sci. Technol*.**, 31**, 063001 (2016).
28. X. Liu, C. Chen, L. Wang, J. Zhong, M. Luo, J. Chen, D.-J. Xue, D. Li, Y. Zhou, J. Tang, *Prog. Photovoltaics: Research and Applications*, **23**, 1828 (2015).
29. Y. Zhou, L. Wang, S. Chen, S. Qin, X. Liu, J. Chen, D.-J. Xue, M. Luo, Y. Cao, Y. Cheng, E.H. Sargent, J. Tang, *Nat. Photon.*, **9**, 409 (2015).
30. M. Leng, M. Luo, C. Chen, S. Qin, J. Chen, J. Zhong, J. Tang, *Appl. Phys. Lett.***, 105**, 083905 (2014).
31. D. Kim, K.K. Sakimoto, D. Hong, P. Yang, *Angew. Chem*., **54**, 3259 (2015).
32. A.Sh. Aliyev, R.G. Guseynova, U.M. Gurbanova, D.M. Babanly, V.N. Fateev, I.V. Pushkareva, D.B. Tagiyev, *Chemical Problems*, **16**, 283 (2018).
33. L.J. Minggu, R.W.D. Wan, M.B. Kassim, *Inter. J. Hydrog. Energy***, 35**, 5233 (2010).
34. Y. Yang, S. Niu, D. Han, T. Liu, G. Wang, Y. Li, *Adv. Energy Mater.*, **7**, 1700555 (2017).
35. T.L. Kulova, I.I. Nikolaev, V.N. Fateev, A.Sh. Aliyev, *Chemical Problems*, **16**, 9 (2018).
36. V.N. Fateev, O.K. Alexeeva, S.V. Korobtsev, E.A. Seregina, T.V. Fateeva, A.S. Grigorev, A.Sh. Aliyev, *Chemical Problems*, **16**, 453 (2018).
37. X. Liu, C. Jie, L. Miao, M. Leng, X. Zhe, Z. Ying, S. Qin, D.J. Xue, L. Lu, H. Han, *Acs Appl. Mater. Interfaces***, 6**, 10687 (2014).
38. R. Venkatasubramanian, E. Silvola, T. Colpitts, B. O'Quinn, *Nature***, 413**, 597 (2001).
39. X. Ou, C. Yang, X. Xiong, F. Zheng, Q. Pan, C. Jin, M. Liu, K. Huang, *Adv. Funct. Mater.*, **27**, 1606242 (2017).
40. L. Zhiqiang, Z. Hongbing, G. Yuting, N. Xiaona, C. Xu, Z. Chong, Z. Wen, L. Xiaoyang, Z. Dong, C. Jingwei, M. Yaohua, *Appl. Phys. Express.***, 9**, 052302 **(**2016).
41. Y. Li, Y. Zhou, J. Luo, W. Chen, B. Yang, X. Wen, S. Lu, C. Chen, K. Zeng, H. Song, J. Tang, *RSC Adv*.**, 6**, 87288 (2016).
42. S. Messina, M.T.S. Nair, P.K. Nair, *J. Electrochem. Soc*.**, 156**, H327 (2009).
43. Y. Rodriques-Lazcano, Y. Peña, M.T.S. Nair, P.K. Nair, *Thin Solid Films*, **493**, 77 (2005).
44. B. Yang, D.-J. Xue, M. Leng, J. Zhong, L. Wang, H. Song, Y. Zhou, J. Tang, *Sci. Rep.***, 5**, 10978 (2015).
45. A.M. Fernández, M.G. Merino, *Thin Solid Films***, 66**, 202 (2000).
46. X. Wang, K.F. Cai, F. Shang, S. Chen, *J. Nanopart. Res.***, 15**, 1541 (2013).
47. L. Yu, J. Chen, Z.-W. Fu. *Electrochim. Acta***, 55**, 1258 (2010).
48. J. Yang, Y. Lai, Y. Fan, Y. Jiang, D. Tang, L. Jiang, F. Liu, J. Li, *RSC Adv.***, 5**, 85592 (2015).
49. P.M. Vyacheslavov, N.M. Shmeleva, Test methods for electrolytic coatings. L.: Engineering, 1977.
50. V.A. Majidzade, P.H. Guliyev, A.Sh. Aliyev, M. Elrouby, D.B. Tagiyev, *J. Mol. Struct.*, **1136**, 7 (2017).
51. A.Sh. Aliyev, M. Elrouby, Z.H. Hasanli, R.H. Huseynova, M.T. Abbasov, *Chemical Problems*, **1**, 62 (2015).
52. V.A. Majidzade, A.Sh. Aliyev, P.H. Guliyev, Y.N. Babayev, M. Elrouby, D.B. Tagiyev, *J. Electrochem. Sci., Eng.***, 8**, 197 (2018).
53. V.A. Majidzade. *Chemical Problems*, **3**, 331 (2018).